

## Supporting Information

### High-capacity cathodes for magnesium lithium chlorine tri-ion batteries through chloride intercalation in layered MoS<sub>2</sub>: a computational study

Zhuo Wang, and Guosheng Shao \*

**Table S1.** Voltages (v.s. Li) and capacities in the Li<sub>x</sub>MoS<sub>2</sub> system

Compositions	Voltage v.s. Li (V)	Capacity (mAhg <sup>-1</sup> )
Li <sub>0.25</sub> MoS <sub>2</sub>	2.5	41.4
Li <sub>0.5</sub> MoS <sub>2</sub>	1.54	82.0
Li <sub>0.75</sub> MoS <sub>2</sub>	1.49	121.6
LiMoS <sub>2</sub>	1.35	160.5
Li <sub>1.5</sub> MoS <sub>2</sub>	0.37	-

**Table S2.** Voltages (v.s. Mg) and capacities in the Mg<sub>x</sub>MoS<sub>2</sub> or hybrid Mg<sup>2+</sup>/Li<sup>+</sup> compounds with stable *dT* structures.

Compositions	Voltage v.s. Mg (V)	Capacity (mAhg <sup>-1</sup> )
Mg <sub>0.25</sub> MoS <sub>2</sub>	0.65	80.7
Mg <sub>0.5</sub> MoS <sub>2</sub>	0.18	155.8
Mg <sub>0.75</sub> MoS <sub>2</sub>	0.06	-
Li <sub>0.25</sub> Mg <sub>0.25</sub> MoS <sub>2</sub>	1.08	119.8
Li <sub>0.5</sub> Mg <sub>0.25</sub> MoS <sub>2</sub>	0.9	160.0

**Table S3.** Voltage (v.s. Mg) and capacities in Li<sub>x</sub>Mg<sub>y</sub>MoS<sub>2</sub>Cl<sub>0.5</sub> compounds with stable *dT* structures.

Compositions	Voltage v.s. Mg (V)	Capacity (mAhg <sup>-1</sup> )
Li <sub>0.5</sub> MoS <sub>2</sub> Cl <sub>0.5</sub>	2.4	147.9
Mg <sub>0.25</sub> MoS <sub>2</sub> Cl <sub>0.5</sub>	1.9	145.9
Li <sub>0.25</sub> Mg <sub>0.25</sub> MoS <sub>2</sub> Cl <sub>0.5</sub>	1.1	180.6
Li <sub>0.5</sub> Mg <sub>0.25</sub> MoS <sub>2</sub> Cl <sub>0.5</sub>	0.92	214.7
LiMoS <sub>2</sub> Cl <sub>0.5</sub>	0.85	217.6
Mg <sub>0.5</sub> MoS <sub>2</sub> Cl <sub>0.5</sub>	0.8	211.9
Li <sub>0.25</sub> Mg <sub>0.5</sub> MoS <sub>2</sub> Cl <sub>0.5</sub>	0.75	244.9
Li <sub>0.5</sub> Mg <sub>0.5</sub> MoS <sub>2</sub> Cl <sub>0.5</sub>	0.67	277.4

**Tables S4** Reported data on performance of different cathode materials.

Material	Electrolyte (mol)	Capacity (mAhg <sup>-1</sup> ) at 0.1C *	Voltage (V)	Morphology
Expanded MoS <sub>2</sub> /graphene	0.25LiCl+0.25APC	300	1.2	Nanosheets <sup>1</sup>
Expanded TiS <sub>2</sub>	0.2PY14Cl+0.25APC	239	0.7	Nanosheets <sup>2</sup>
TiS <sub>2</sub>	0.1Mg(BH <sub>4</sub> ) <sub>2</sub> + 1.0NaBH <sub>4</sub>	200	~1.1	Nanosheets <sup>3</sup>
MoS <sub>2</sub>	1LiCl+0.4APC	243	1.1	Nanoflakes <sup>4</sup>
TiO <sub>2</sub>	1.5LiBH <sub>4</sub> +0.5Mg(BH <sub>4</sub> ) <sub>2</sub> /TG	140	1.15	Nanoparticles <sup>5</sup>
Li <sub>4</sub> Ti <sub>5</sub> O <sub>12</sub> /Graphene	1.5LiBH <sub>4</sub> +0.4APC	147.5	~1.1	Micron-sized particles <sup>6</sup>
Mo <sub>6</sub> S <sub>8</sub>	0.4LiCl+1APC	126	~1.7	Particles <sup>7</sup>
Ti <sub>3</sub> C <sub>2</sub> T <sub>x</sub> /CNT	0.4LiCl+0.5APC	105	-	Micron-sized delaminated flakes <sup>8</sup>

\* Reported experimental data were based on active cathode (e.g. sulphide) materials in composite cathodes.

1.X. Fan, R. R. Gaddam, N. A. Kumar and X. S. Zhao, *Adv. Energy Mater.*, 2017, 1700317.

2. H. D. Yoo, Y. Liang, H. Dong, J. Lin, H. Wang, Y. Liu, L. Ma, T. Wu, Y. Li, Q. Ru, Y. Jing, Q. An, W. Zhou, J. Guo, J. Lu, S. T. Pantelides, X. Qian and Y. Yao, *Nat. Commun.*, 2017, **8**, 339.

3.X. Bian, Y. Gao, Q. Fu, S. Indris, Y. Ju, Y. Meng, F. Du, N. Bramnik, H. Ehrenberg and Y. Wei, *J. Mater. Chem. A*, 2017, **5**, 600-608.

4.Yanming Ju, Yuan Meng, Yingjin Wei, Xiaofei Bian, Qiang Pang, Yu Gao, Fei Du, Bingbing Liu and G. Chen, *Chem. Eur. J.*, 2016, **22**, 18073 – 18079.

5. S. Su, Z. Huang, Y. NuLi, F. Tuerxun, J. Yang and J. Wang, *Chem. Commun.*, 2015, **51**, 2641-2644.

6. Q. Miao, Y. NuLi, N. Wang, J. Yang, J. Wang and S.-i. Hirano, *RSC Advances*, 2016, **6**, 3231-3234.

7. Y. Cheng, Y. Shao, J. G. Zhang, V. L. Sprenkle, J. Liu and G. Li, *Chem. Commun.*, 2014, **50**, 9644--9646.

8. A. Byeon, M. Q. Zhao, C. E. Ren, J. Halim, S. Kota, P. Urbankowski, B. Anasori, M. W. Barsoum and Y. Gogotsi, *ACS Appl. Mater. Interfaces*, 2017, **9**, 4296-4300.

**Figure S1** Low energy structural configurations from USPEX global searching: (a) single layer MoS<sub>2</sub> (2H phase), (b) Li<sub>0.5</sub>MoS<sub>2</sub>, (c) LiMoS<sub>2</sub>, (d) Mg<sub>0.25</sub>MoS<sub>2</sub>, (e) Mg<sub>0.5</sub>MoS<sub>2</sub>, (f) Li<sub>0.5</sub>Mg<sub>0.25</sub>MoS<sub>2</sub>, and (g) Li<sub>0.25</sub>Mg<sub>0.5</sub>MoS<sub>2</sub>. (b-g) exhibit characteristic layered structure of dT phases.

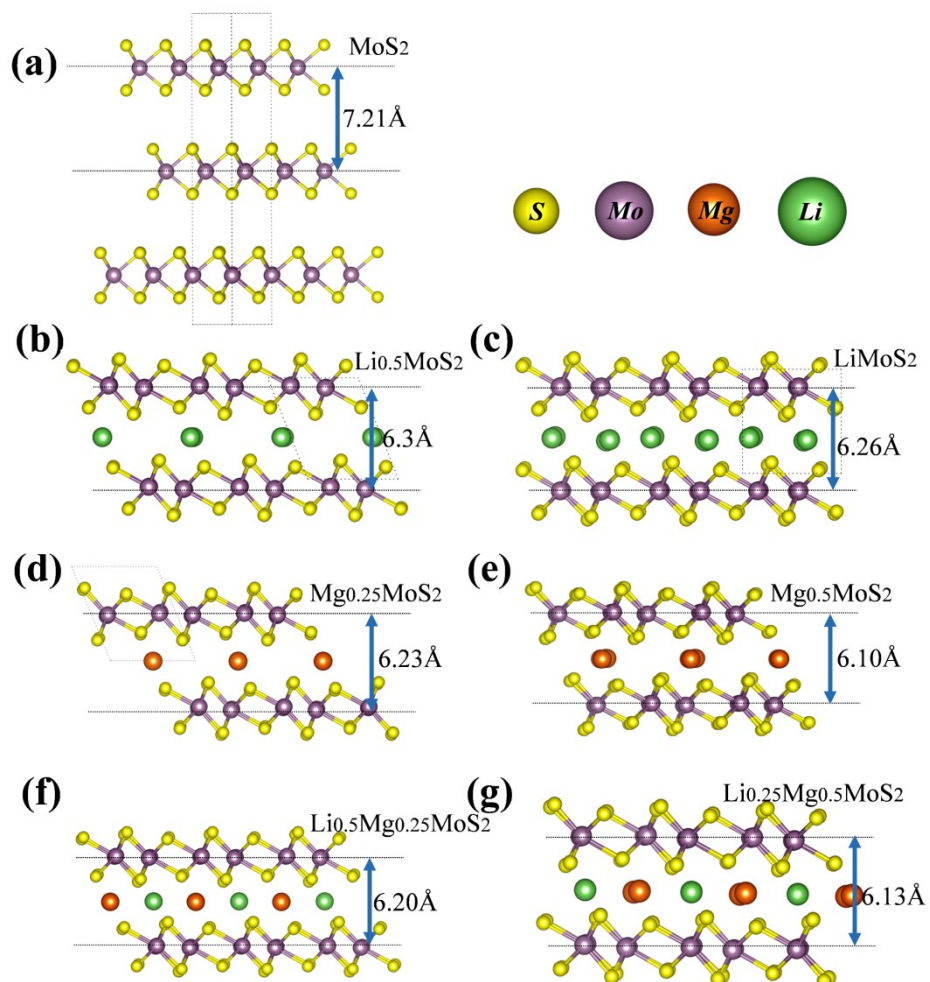


**Figure S2** Low-energy structural configurations from USPEX global searching, for (a)  $\text{Li}_{1.5}\text{MoS}_2$ , (b)  $\text{Li}_{0.5}\text{Mg}_{0.5}\text{MoS}_2$ , and (c)  $\text{Mg}_{0.75}\text{MoS}_2$ . Higher level of intercalation of alkali and/or alkali-earth metal ions leads to loss of layered structures.

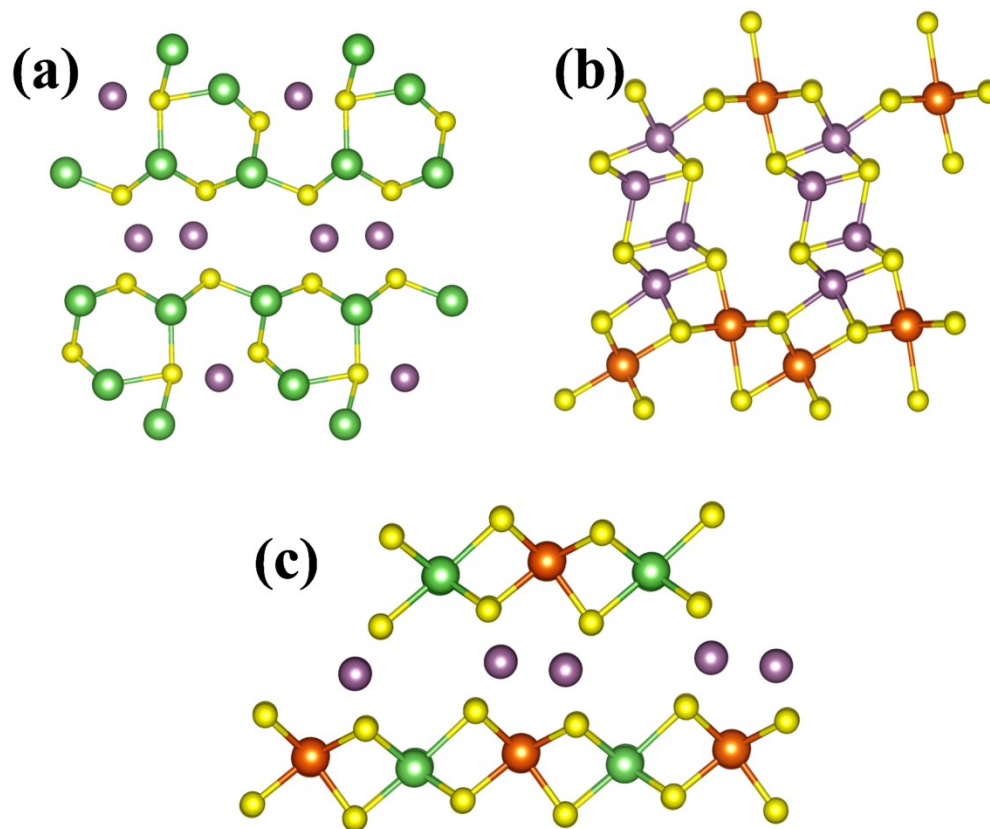


**Figure S3** Reference AIMD simulation for the well-established LIB cathode  $\text{LiCoO}_2$ : (a) Layered structure of  $\text{LiCoO}_2$ , (b)  $\text{Li}^+$  diffusion coefficient in  $\text{LiCoO}_2$ , and (c) trajectory map of  $\text{Li}^+$  ions from the particle density distribution at 1200K.

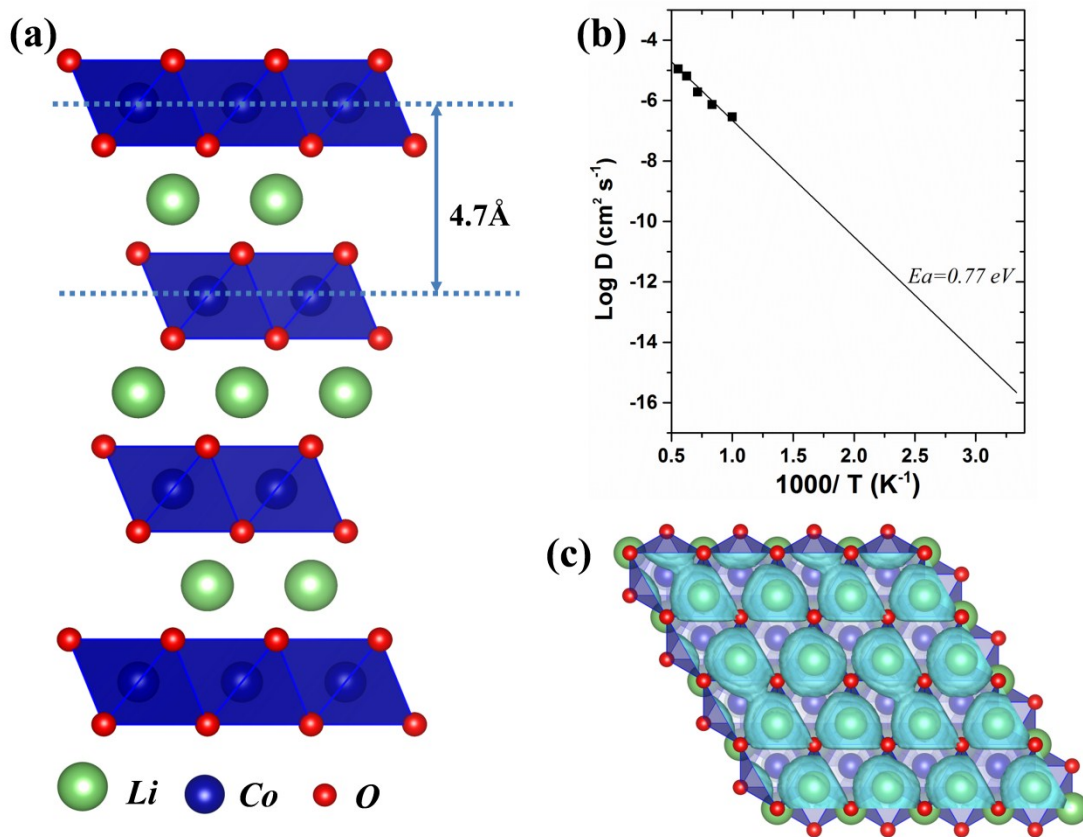


**Figure S4** The trajectory of ions from AIMD at 1200K from the particle density distribution: Trajectories of (a)  $\text{Cl}^-$  and (b)  $\text{Mg}^{2+}$  in  $\text{Mg}_{0.5}\text{MoS}_2\text{Cl}_{0.5}$ ; Trajectories of (c)  $\text{Cl}^-$ , (d)  $\text{Mg}^{2+}$ , and (e)  $\text{Li}^+$  in  $\text{Li}_{0.25}\text{Mg}_{0.25}\text{MoS}_2\text{Cl}_{0.5}$ .

